

BOUNDARY LAYER STATE AND FLOW FIELD STRUCTURE ON WIND TURBINE BLADES

Horia DUMITRESCU*, Maria ALEXANDRESCU**, Nicusor ALEXANDRESCU**

* Institute of Statistics and Applied Mathematics, Bucharest

** "Elie Carafoli" Aerospace National Institute, 220 Iuliu Maniu Street, Bucharest
Corresponding author: Horia DUMITRESCU, hdumitrescu@gheorghita.ro

Blade rotation routinely and significantly augments aerodynamic forces during zero yaw horizontal axis wind turbine operation. To better understand the flow physics underlying this phenomenon, three-dimensional and rotational viscous effects on wind turbine blades are investigated by means of 3-D boundary layer model. The governing equations of the model are derived from 3-D primitive variable boundary-layer equations written in cylindrical coordinates in the rotating frame of reference. The latter are integrated along the peripheral direction with the radial distance as parameter for a particular external flow. The skin friction coefficient is used to identify boundary layer separation and shear layer reattachment locations. Separation and reattachment kinematics shows at inboard locations that while the separation point location is not really affected and remains near the leading edge, the reattachment point advances forward rapidly on the blade chord from the trailing edge as radial distance decreases. It is concluded that the rotational augmentation is linked to specific separation and reattachment state strictly determined by the Coriolis forces..

Key words: Wind turbine, flow field, boundary layer, separation, reattachment, Coriolis force

1. INTRODUCTION

Flow fields generated by horizontal axis wind turbines (HAWT) are highly complex due to the simultaneous presence and interaction of three- dimensionality, unsteadiness, separation, reattachment and rotational influences. Both previous theoretical computations and experiments established that dynamic stall routinely occurs on HAWT blades, producing beneficial vortex structures responsible for significant force and moment amplifications [1-5]. However, rotational influences remain incompletely characterized and understood, particularly at inboard locations.

The widely cited experiments of Himmelskamp [6] indicate that stall delay and lift augmentation due to rotation, with lift coefficients as high as 3 near the hub, were found for a fan blade. To explain these results, radial thinning and chordwise acceleration of the steady boundary layer, due to centrifugal and Coriolis forces, were postulated. A complementary theoretical analysis was performed by Banks and Gadd [7] for steady laminar boundary layers on a rotating blade using an integral method and an external flow with a linear adverse velocity gradient. They concluded that rotational effects could delay the separation, and at extreme inboard stations could stabilize completely the boundary layer against separation. More recent, in a technical note Dumitrescu and Cardos [8] using a differential boundary-layer formulation with the same linearly retarded external flow, found similar results and nominated the Coriolis forces occurring in the separated flow as the main cause for stall-delay and increased 3-D post stall lift coefficients. However, the transition mechanisms from the separated flow regime, at outboard locations, to the attached flow regime at inboard locations, remained incompletely characterised and understood,

Attempts have been made mentioned to investigate this phenomenon using both CFD tools and full-scale HAWT experiments but they either were limited to large values of the radius to local chord ratio ($r/c > 3$) [1,2], or were affected by experimental uncertainties of separation and/or reattachment detection criteria [3]. Thus there is a need for a analysis method which is computationally reasonable at the same time

as it is capable of predicting leading 3-D effects on a rotating blade in attached as well as in stalled conditions.

2. SEPARATION AND ATTACHMENT OF 3-D BOUNDARY LAYER

A three-dimensional boundary layer starts from either a line or point on the surface, called a line or point of attachment. It is an experimental fact that after following the surface for some distance the boundary layer separates and forms a region of reversed flow on the surface and a wake behind the surface. The main difficulty in evolving a comprehensive theory of this subject is that the conditions under which a 3-D boundary layer separation occurs are many and varied. The case considered here is comprised in the category of boundary layers separated under combined effects of viscosity and adverse pressure gradient. We shall exclusively be concerned with the steady-state boundary layers on developable surfaces (characterized by zero total curvature at any point on surface).

Referring to the equations of a boundary layer on a rotating developable surface in Cartesian form we have:

$$\frac{\partial u}{\partial x} + \frac{\partial v}{\partial y} + \frac{\partial w}{\partial z} = 0 \quad (1)$$

$$u \frac{\partial u}{\partial x} + v \frac{\partial u}{\partial y} + w \frac{\partial u}{\partial z} - 2\Omega v = -\frac{1}{\rho} \frac{\partial}{\partial x} \left(p_e - \rho \frac{\Omega^2}{2} \right) + v \frac{\partial^2 u}{\partial y^2} \quad (2)$$

$$u \frac{\partial v}{\partial x} + v \frac{\partial v}{\partial y} + w \frac{\partial v}{\partial z} + 2\Omega u = -\frac{1}{\rho} \frac{\partial}{\partial y} \left(p_e - \rho \frac{\Omega^2}{2} \right) + v \frac{\partial^2 v}{\partial z^2} \quad (3)$$

Where u, v and w are the velocity components along x, y and z , respectively, $(Oxyz)$ is the rotating reference system associated with constant angular velocity Ω about the z -axis and Oy define the spanwise direction of the blade (Fig.1).

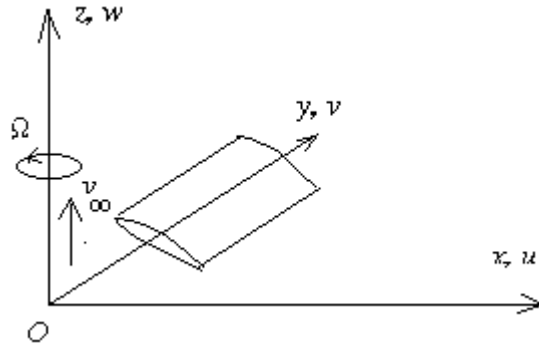


Figure 1. Definition of the coordinates

At the surface $z=0$, because of the no-slip condition, $u = v = w = 0$. Denoting the viscous shear stress at the wall by τ_{Ox} and τ_{Oy} defined as

$$\tau_{Ox} = \mu \left(\frac{\partial u}{\partial z} \right)_0, \quad \tau_{Oy} = \mu \left(\frac{\partial v}{\partial z} \right)_0 \quad (4)$$

we expand each velocity component near the wall by Taylor's expansion to have:

$$u = \frac{z\tau_{Ox}}{\mu} + O(z^2) \quad (5a)$$

$$v = \frac{z\tau_{Oy}}{\mu} + O(z^2) \quad (5b)$$

$$w = -\frac{z^2\Delta}{2\mu} + O(z^3) \quad (5c)$$

where $\Delta = \frac{\partial\tau_{Ox}}{\partial x} + \frac{\partial\tau_{Oy}}{\partial y}$, and μ is the coefficient of viscosity. Based on Eqs.(5) we conclude that if at a point both wall shear stresses τ_{Ox} and τ_{Oy} are not simultaneously zero, then:

$$\lim_{z \rightarrow 0} \frac{w}{\sqrt{u^2 + v^2}} \rightarrow 0 \quad (6)$$

Therefore, w is a lower order of magnitude than either u or v . All those points on the surface where Eq.(6) holds are known as the regular points of the flow. Note that if one of the wall shear stresses is zero then the point is still a regular point of the flow. However, if both the wall shear stresses vanish simultaneously at a point on the surface, then:

$$\lim_{z \rightarrow 0} \frac{w}{\sqrt{u^2 + v^2}} \rightarrow O(1) \quad (7)$$

and then the velocity component w is of the same order as the other two. Points in the surface where Eq.(7) holds are called the singular points of the flow.

In the event of a singularity at a point two cases arise depending on the sign of Δ . Referring to Eq.(5c) we find that if $\Delta < 0$, then the fluid will leave the surface at an angle; while if $\Delta > 0$, then the boundary layer attaches itself to the surface. From this result we conclude that in three dimensions reattachment is as important as separation. In either case, simultaneous vanishing of τ_{Ox} and τ_{Oy} give rise to either separation or reattachment of the flow. This condition is satisfied, in general, at isolated points of the surface, but in some particular circumstances (such as in two-dimensional flows) both wall shear stresses vanish all along a line and then we have a line of separation or reattachment.

The equations of a streamline in the flow are:

Therefore, the streamlines in the surface are given by:

$$\begin{aligned} \frac{dx}{u} &= \frac{dy}{v} = \frac{dz}{w} \\ \frac{dx}{dy} &= \lim_{z \rightarrow 0} \frac{u}{v} \end{aligned} \quad (8)$$

and are called the limiting streamlines. Using Equations 5a,b in equations (8) we find that the differential equation for the limiting streamlines as:

$$\frac{dx}{\tau_{Ox}} = \frac{dy}{\tau_{Oy}} \quad (9')$$

or, alternatively:

$$\frac{dx}{\tau_x} = \frac{dy}{\tau_y}, \quad z = 0 \quad (9'')$$

From Equations (8) and (9) we conclude that a limiting streamline is a curve whose directions coincide with that of the vanishing fluid velocity or the shear stress, at the surface.

In the same manner, the differential equation for vortex lines in the surface is obtained by evaluating the vorticity components at the surface to have:

$$\frac{dx}{\omega_{Ox}} = \frac{dy}{\omega_{Oy}} \quad (10)$$

where:

$$\omega_{0x} = -\frac{\tau_{0y}}{\mu} \quad \text{and} \quad \omega_{0y} = \frac{\tau_{0x}}{\mu}$$

In vector form, the differential equations of the limiting streamlines and vortex lines in the surface respectively are:

Since:

$$d\vec{r} \times \vec{\tau}_0 = 0, \quad d\vec{r} \times \vec{\omega}_0 = 0, \quad \vec{\tau}_0 \cdot \vec{\omega}_0 = 0 \quad (11)$$

both systems of lines cover the surface completely and intersect each other orthogonally. At a regular point there is just one limiting streamline intersecting one surface vortex line. In the situation when $\tau_{0x} = \tau_{0y} = 0$, the point is a singular or branch point of both the differential equations (Eqs. (11)). A classification of such branch point [9] is conducted by studying sign of the Jacobian J defined as:

$$J = \frac{\partial \omega_{Oy}}{\partial y} \frac{\partial \omega_{Ox}}{\partial x} - \frac{\partial \omega_{Ox}}{\partial x} \frac{\partial \omega_{Oy}}{\partial y} = \left(\frac{\partial \tau_{0y}}{\partial y} \frac{\partial \tau_{0x}}{\partial x} - \frac{\partial \tau_{0x}}{\partial x} \frac{\partial \tau_{0y}}{\partial y} \right) / \mu^2$$

If $J < 0$ then the singular point is a saddle point; if $J > 0$ then the singular point is a nodal point; and if $J = 0$ then the singular point is a focus.

On the basis of the above results, we can form a conceptual model of the separation phenomenon as follows. In the event of simultaneous vanishing of both wall shear stresses at a point or a group of points on the surface, there exists a separated region which is inaccessible to the viscous upstream region. The two regions are separated by a surface called the separation surface. It is generally admitted that separation surfaces may be divided in two types: the bubble type and the free-shear layer type, (ordinary separation). The trace of curve of the intersection of separation surface with the body is a separation or reattachment line. Since no limiting streamline can pass through the separation line, the separation line must be the envelope of limiting streamlines. On the separation or reattachment line there are singular points, i.e. points which belong to both the separated and unseparated regions. These points are the branch points (saddle, nodal or focus points), at which the velocity component normal to the surface is of the same order as the other two components; therefore the boundary layer leaves or attaches to the surface.

3. THE 3-D BOUNDARY-LAYER MODEL

A simple 3D boundary-layer model has been devised in order to identify the influence of the three-dimensional and rotational effects on the blade section characteristics. The governing equations are derived using the following steps:

Step 1: The 3D incompressible steady boundary layer equations are written in the cylindrical coordinate system (θ, r, z) which rotate with the blade with a constant rotational speed Ω (fig.2) [8]. θ denotes the peripheral, z the axial and r the radial (blade spanwise) direction. The infinitesimal length in the peripheral direction is $dx = r d\theta$. The equations one used here in their laminar form:

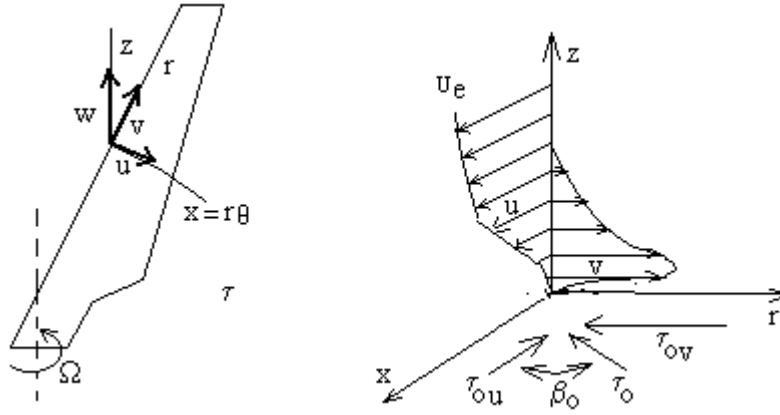


Figure 2. Cylindrical coordinate system fixed to the rotating blade, nature of chordwise (u) and spanwise (v) velocity profiles

Continuity:

$$\frac{1}{r} \frac{\partial u}{\partial \theta} + \frac{\partial w}{\partial z} + \frac{\partial v}{\partial r} + \frac{v}{r} = 0 \quad (12)$$

Momentum, θ component:

$$\frac{u}{r} \frac{\partial u}{\partial \theta} + w \frac{\partial u}{\partial z} + v \frac{\partial u}{\partial r} - \frac{v}{r} (2\Omega r - u) = -\frac{1}{r} \frac{\partial P}{\partial \theta} + \nu \frac{\partial^2 u}{\partial z^2} \quad (13)$$

Momentum, r component:

$$\frac{u}{r} \frac{\partial v}{\partial \theta} + w \frac{\partial v}{\partial z} + v \frac{\partial v}{\partial r} + \frac{u}{r} (2\Omega r - u) = -\frac{1}{r} \frac{\partial P}{\partial r} + \nu \frac{\partial^2 v}{\partial z^2} \quad (14)$$

where u , v and w stands for velocity components in θ , r and z directions, respectively, r is the local radius measured from the center of rotation, ρ is the fluid density and ν the kinematic viscosity, P is a pressure like term including the centrifugal effect:

$$P = \frac{p_e}{\rho} - \frac{1}{2} (\Omega r)^2 \quad (15)$$

Step 2: The above system of equations is subjected to the following assumptions:

By considering the flow around an infinite cylinder of arbitrary cross-section rotating steadily about the z -axis, Fig.1, it is shown by Sears [10] that the inviscid velocity components may be written as:

$$u_e = \Omega r \frac{\partial \phi}{\partial x} \quad ; \quad v_e = \Omega [\phi - 2x] \quad ; \quad w_e = \Omega r \frac{\partial \phi}{\partial z} \quad (16)$$

where $\phi = \phi(x, z)$ denotes the equivalent 2D velocity potential due to a blade in translational movement with

$$\left(u_e^2 + w_e^2 \right)^{1/2} / (\Omega r)$$

unit speed in the negative x -direction. Thus the inviscid chordwise velocity distribution, is found to be the same at wall spanwise positions. This is a plausible approximation that allows us to include the important effects of Coriolis and centrifugal forces only in the three-dimensional boundary layer equations as additional terms. This similarity assumption was also used in a few Navier-Stokes models [1,2].

To derive an extended 3D boundary layer approach, capable of predicting leading rotational and 3D effects in attached as well as in stalled conditions, a zero skin friction flow (hereafter called Stratford flow) is

assumed to describe the inviscid external flow after separation. This obviously introduces deviations, as compared to a fully separated flow, but they are not significant as long as this approximation allows us to obtain a better understanding of the 3D separation topology on a rotating blade. Therefore, the Eqs.(12-15) are solved for a particular external flow represented by a two flow fields:

- an attached flow field given by

$$U = U_{\infty} \left(1 - k \frac{x}{c}\right) = \sqrt{V_w^2 + (\Omega r)^2} \left(1 - k \frac{x}{c}\right) \quad \text{for } \frac{x}{c} \leq \left(\frac{x}{c}\right)_{sep} \quad (17)$$

where c is the chord length and V_w the wind velocity.

- a separating(zero skin friction) flow field given by the Stratford's criterion [11]

$$C_p \left(x \frac{dC_p}{dx}\right)^2 = \left[C_p \left(x \frac{dC_p}{dx}\right)^2 \right]_s = \text{const.}, \quad \text{for } \frac{x}{c} \geq \left(\frac{x}{c}\right)_s \quad (18)$$

where

$$C_p = \frac{p - p_{\infty}}{\frac{1}{2} \rho U_{\infty}^2} = 1 - \left(\frac{U}{U_{\infty}}\right)^2 = k \left(\frac{x}{c}\right) (2 - k \frac{x}{c})$$

and the value of

$$\left[C_p \left(x \frac{dC_p}{dx}\right)^2 \right]_s$$

at separation for such external linearly retarded flows is 0.01. Figures 3 and 4 show chordwise inviscid velocity distributions and the variations of peripheral skin-friction coefficient for various values of the velocity gradient parameter, k , and $r/c = \infty$ (2D).

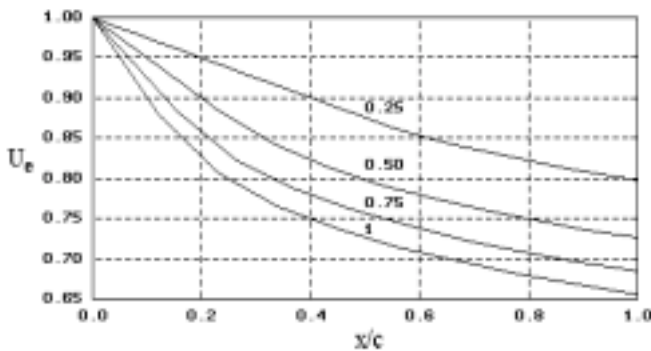


Figure.3. External velocity distributions for various velocity gradients k

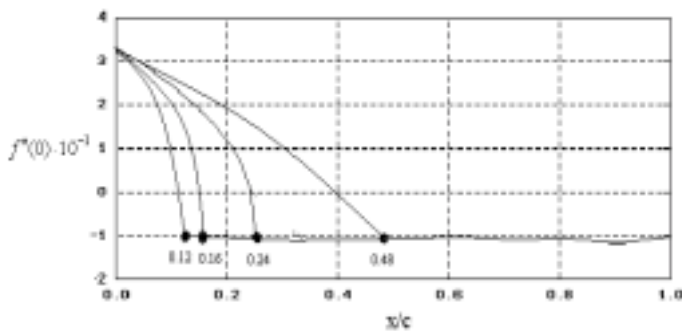


Figure 4. Chordwise skin- friction coefficients for various external velocity distributions (• separation point)

In many cases, the linear adverse velocity gradient assumption is a satisfactory approximation to the real operating condition and can be used for simulating the velocity distribution on the upper surface of wind turbine blade. The extension of this flow type after separation with distributions that maintain a separating flow state (incipient detachment) allows us further to use the boundary layer model for this complex analysis. Thereby, it is implicitly suppose that the flow field structure underlying rotational augmentation of blade aerodynamic loading is not qualitatively affected by Reynolds number.

Step 3: The outcome of the analysis is the set of equations (12-15) including Eqs.(17,18) for computing of the pressure derivatives.

As described in Ref.[8] the Blasius parameters are used

$$\xi = x/c = \frac{r}{c}\theta, \quad \eta = z\sqrt{U/xv} \quad (19)$$

and the velocity profiles in boundary layer are defined

$$\frac{u}{U} = \frac{\partial f}{\partial \eta} = f'(\xi, \eta), \quad \frac{v}{U} = \frac{\partial g}{\partial \eta} = g'(\xi, \eta) \quad (20)$$

Then with ξ and η as independent variables, substitute expressions (19) and (20) into Eqs. (12-15) to obtain:

$$\begin{aligned} f''' + \frac{1}{2} \left(f + 2\xi f_\xi + 2\frac{c}{r}\xi g \right) f'' - \xi f'_\xi f' + \frac{c}{r} \frac{1}{U} \frac{\partial U}{\partial \theta} \xi \left(1 + \frac{1}{2} f f'' - f'^2 \right) + \\ \frac{c}{U} \frac{\partial U}{\partial r} \xi \left(\frac{1}{2} f'' g - f' g' \right) + \frac{c}{r} \xi g' \left(\frac{2\Omega r}{U} - f' \right) = 0 \end{aligned} \quad (21)$$

$$\begin{aligned} g''' + \frac{1}{2} \left(f + 2\xi f_\xi + 2\frac{c}{r}\xi g \right) g'' - \xi g'_\xi f' + \frac{c}{r} \frac{1}{U} \frac{\partial U}{\partial \theta} \xi \left(\frac{1}{2} f g'' - f' g' \right) + \\ \frac{c}{U} \frac{\partial U}{\partial r} \xi \left(1 + \frac{1}{2} g g'' - g'^2 \right) - \frac{c}{r} \xi f' \left(\frac{2\Omega r}{U} - f' \right) = 0 \end{aligned} \quad (22)$$

The boundary conditions are:

$$\begin{aligned} \eta = 0, \quad f(\xi, 0) = 0, \quad f'(\xi, 0) = 0 \\ g(\xi, 0) = 0, \quad g'(\xi, 0) = 0 \end{aligned} \quad (23)$$

$$\eta \rightarrow \infty, \quad f'(\infty) = 1, \quad g'(\infty) = 0 \quad (24)$$

where the prime denotes differentiation with respect to η and subscript ξ the differentiation with respect to ξ .

The skin-friction coefficients are given by

$$\frac{1}{2} C_{f,u} \text{Re}_x^{1/2} = f_0'', \quad \frac{1}{2} C_{f,v} \text{Re}_x^{1/2} = g_0'' \quad (25)$$

The coupled partial differential equation given by Eqs.(21) and (22) under boundary conditions (23),(24) are solved numerically by use of a standard finite difference method [12].

4. RESULTS AND DISCUSSION

In the following, results for laminar is boundary layer flow and particular external flow class are presented. The results obtained for the chordwise and spanwise velocity profiles and skin-friction

coefficients in the separating flow region, at different values of non-dimensional spanwise distance, r/c , are used to detect and track boundary layer separation and reattachment. The pattern of separation and attachment lines suggests the presence of a conical bubble in the inner part of the blade and a free-share layer in the outer part of the blade.

The chordwise velocity profiles in the separated region are shown in fig.5.(left side) From the figure it is seen that, except for a small difference, at all locations r/c , the curves are almost identical with the typical velocity profile at separation.

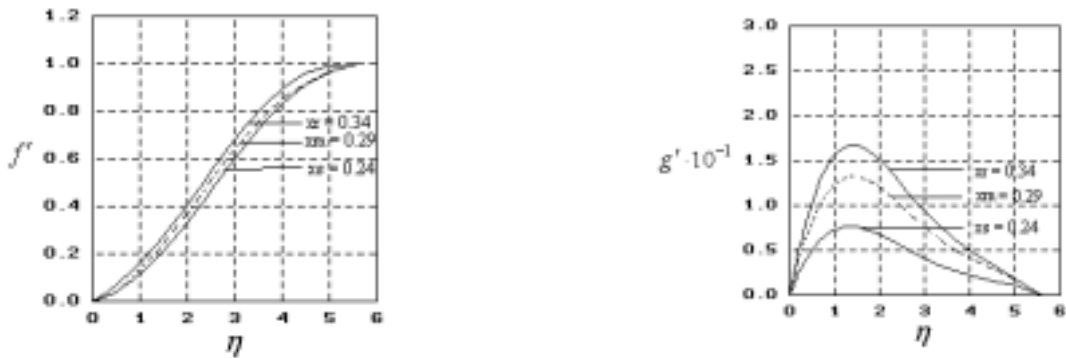
In Fig.5 (right side) where spanwise velocity profiles are shown at varying distances from the rotational axis, r/c , an increase of the velocities (and implicitly of Coriolis forces) is seen in the separated flow region for decreasing r/c .

Distributions of the chordwise skin-friction coefficient, $f''(0)$, and spanwise skin-friction coefficient, $g''(0)$ are in Fig.6 shown at various spanwise distances, r/c . A decrease is seen in the size of separated region, (the distance between the separation and reattachment locations) for decreasing r/c . Since the skin-friction coefficients have small vanishing values, the separation and reattachment locations are identified in conjunction with the steepest skin friction gradient

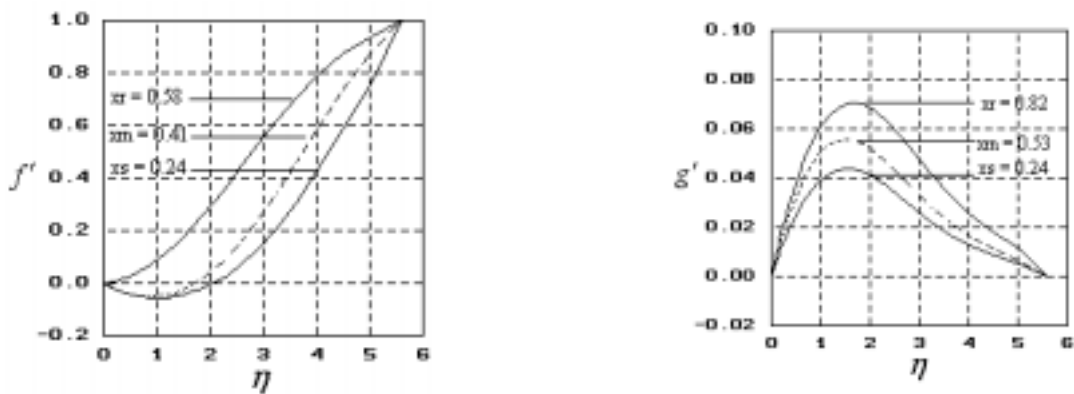
Figure 7 shows the main singular limiting lines joining the different singular points selected from Fig.6.

These lines are: the separation line SL ending at the focus F1, nearly parallel to the leading edge, and the reattachment line RL emerging from the trailing edge and ending at the focus F2. It is possible to assume that these two points are in fact only one singular point, but in order to simplify the construction of the friction lines, it is postulated that these two singular points are distinct. Generally a focus is associated with a rotation of the fluid and consequently with the formation of the vortex sheet which here rolls up into a conical bubble under the Coriolis force action. At a certain location, in the outer part of the blade, where the strength of Coriolis force decreases, the conical sheet unfolds as a free-share layer. The presence of such atationary rolling vortex structure can be responsible for aerodynamic force augmentation on stalled rotating wind turbine blades.

$r/c = 1.95$



$r/c = 5$



$r/c = 9.25$

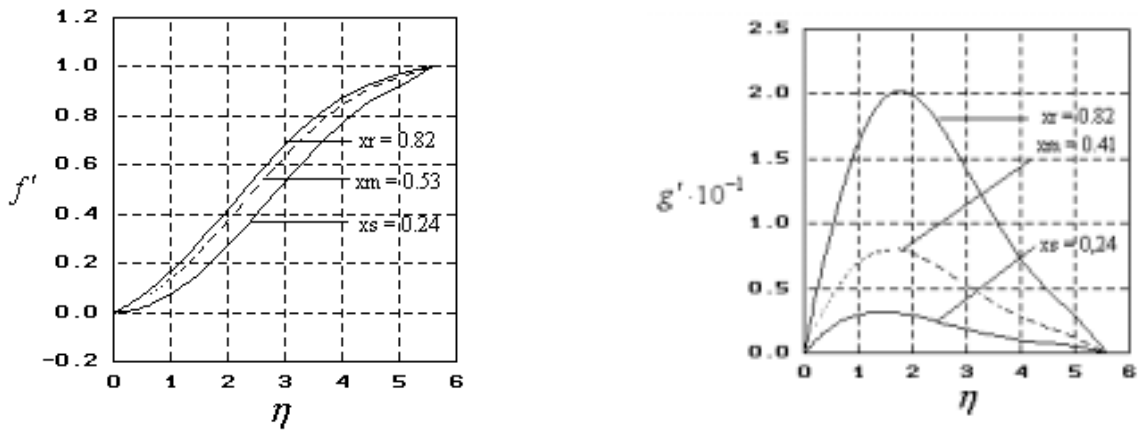
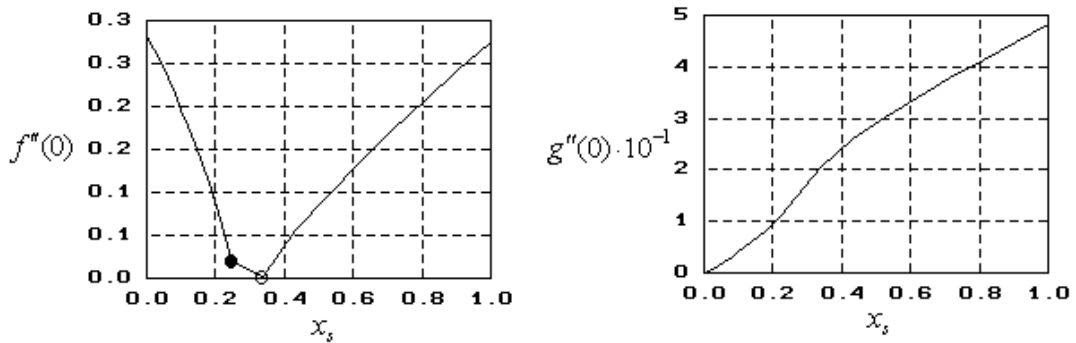
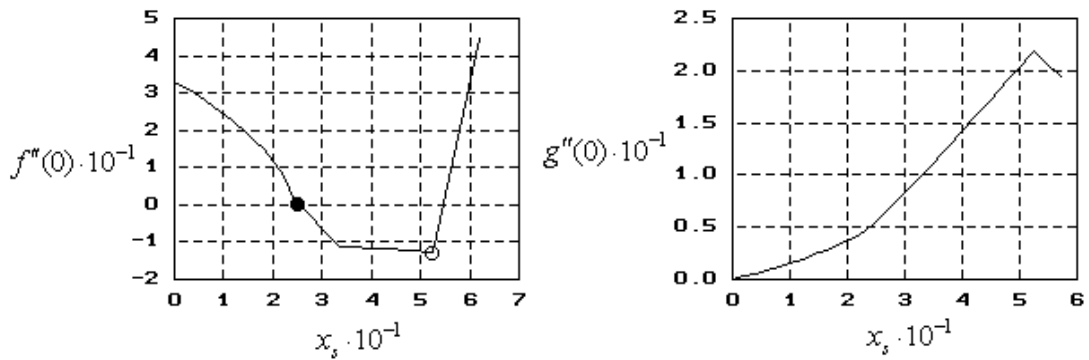


Figure 5. Chordwise (f') and spanwise (g') velocity profiles in the separating boundary layer at three locations separation reattachment and half distance between first two locations, for various ratios r/c

$r/c = 1.9$



$r/c = 5$



$r/c = 9.25$

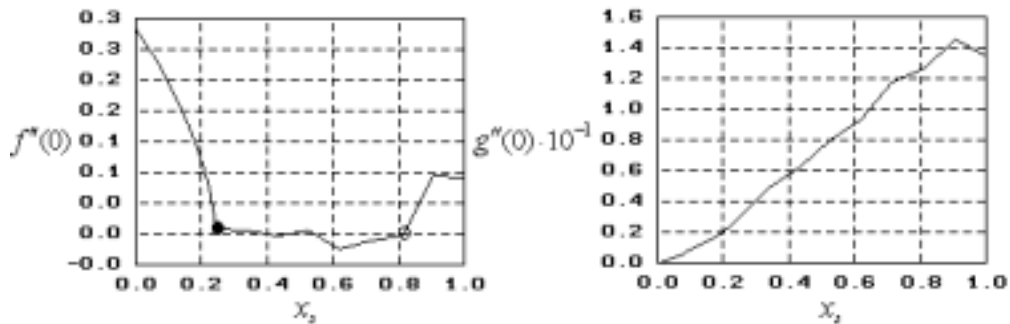


Figure 6. Chordwise (f''_0) and spanwise (g''_0) skin-friction coefficients for various ratios r/c (• separation point; ° reattachment point)

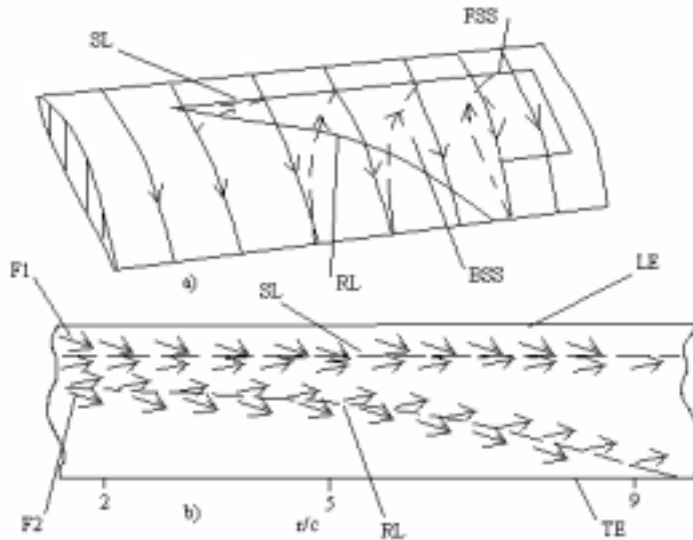


Figure 7. Topological structures of separation on rotating blade, ($k = 0.5$): a) types of separation surface, b) separation reattachment contour

5. CONCLUSIONS

A 3D boundary layer model which takes into account rotational and 3D effects has been developed. The model enables the study of the rotation effect of a rotor blade at very low computing costs. The model shows that rotational effects have an influence on the boundary layer state on blade that depends on the non-dimensional spanwise distance, r/c . Thus, the effect of rotation, which becomes more pronounced at inboard locations, is to suppress vortex shedding and the development of separation bubbles. Results presented indicate that when the flow separates the Coriolis force acts as a favourable pressure gradient which reattaches the flow and reduce the volume of the separation bubble.

The reduction of the bubble volume produces a pressure drop along the suction side of the airfoils increasing, thus, the blade loading.

Also, the results show that the model is capable of determining correctly the qualitative boundary layer state for rotating blades, including the prediction of 3D surface flow field structures.

REFERENCES

1. SHEN, W.Z., SOERENSEN, J.N., *Quasi-3D Navier-Stokes Model for a Rotating Airfoil*, Journal of Computational Physics, **150**, pp. 518-548, 1999.
2. CHAVIAROPOULOS, P.K., HANSEN, M.O.L., *Investigating Three-Dimensional and Rotational Effects on Wind Turbine Blades by Means of a Quasi-3D Navier-Stokes Solver*, Journal of Fluids Engineering (ASME), Vol. **122**, pp. 330-336, 2000.
3. SCHRECK, S., ROBINSON, M., *Boundary Layer State and Flow Field Structure Underlying Rotational Augmentation of Blade Aerodynamic Response*, Journal of Solar Energy Engineering (ASME), vol **125**, pp.448-456, 2003.
4. SCHRECK, S., ROBINSON, M., *Rotational Augmentation of Horizontal Axis Wind Turbine Blade Aerodynamic Response*, Wind Energy, **5**(2/3), pp.133-150, 2002.
5. HUYER, S., SIMMS, D., ROBINSON, M., *Unsteady Aerodynamics Associated with a Horizontal Axis Wind Turbine*, AIAA Journal, **34** (7), pp. 1410-1419, 1996.
6. HIMMELSKAMP, H., *Profile Investigation on a Rotating Airscrew*, Techni. Rep.Ph.D.Diss., Gottingen, Germany, 1945.
7. BANKS, W.H.H., GAAD, G.E., *Delaying Effect of Rotation on Laminar Separation*, AIAA Journal, vol. **1**, No.4, pp.941-942, 1963.
8. DUMITRESCU, H., CARDOS, V., *Rotational Effects on the Boundary Layer Flow in Wind Turbines*, AIAA Journal, vol. **42**, No.2, pp.408-411, 2004.
9. TOBAK, M., PEAKE, D.J., *Topology of Three-Dimensional Separated Flows*, Ann. Rev.Fluid Mech., **14**, pp.61-85, 1984.
10. SEARS, W. R., *Potential Flow Around a Rotating Cylindrical Blade*, Journal of the Aeronautical Sciences, **17** (3), 183-184, 1950.
11. STRATFORD, B. S., *The Prediction of Separation of the Turbulent Boundary Layer*, J. of Fluid Mechanics, **5**, pp. 1-16, 1959.
12. CEBECI, T., COUSTEIX, J., *Modelling and Computation of Boundary-Layer Flows*, Springer-Verlag, Berlin, pp. 381-393, 1999.